Research Article

An immersion and invariance based input voltage and resistive load observer for DC–DC boost converter

Milad Malekzadeh[1] · Alireza Khosravi[1] · Mehdi Tavan[2]

Received: 11 November 2019 / Accepted: 9 December 2019 / Published online: 13 December 2019

Abstract
In this paper, a new nonlinear observer is presented for DC–DC boost converter using immersion and invariance (I&I) technique. The proposed nonlinear observer is easy to implement, simple to tune and realizes global exponential convergence of the estimation error to zero. It is assumed that the input voltage and output load of converter are unavailable and the I&I observer is designed to estimate unavailable parameters using output voltage and inductor current information. Considering optimal performance of observer, an improved particle swarm optimization algorithm is employed to determine observer gains. The search space of parameters in the proposed optimization algorithm is modified and according to this modification, the weak parameters is eliminated and the new parameters are defined for optimization process instead of them. In order to validate the effectiveness of the proposed observer, the practical test is implemented and the experimental results confirm the efficiency of the proposed I&I observer.

Keywords DC–DC boost converter · Immersion and invariance · Observer · Exponential stability · IPSO

1 Introduction

Nowadays, DC–DC power converters are employed to increase or decrease output voltage in various applications of power electronic. Providing reliable voltage with acceptable regulation is one of the topics studied by researchers in recent years [1, 2]. One of the most widely used converters in this field is DC–DC boost converter that is used to regulate the output voltage of systems requiring higher voltage levels. Therefore, this converter is applied in renewable energy sources such as solar energy [3], fuel cell [4] and hybrid vehicles [5]. So, designing an appropriate control scheme that leads to enhance the voltage regulation quality is one of the most important problems in industry. Due to its switching action, the dynamic of this converter is nonlinear. Also, DC–DC boost converter inherits a right-half-plane zero which can give rise to transient response oddities [6, 7]. Moreover, there is a constraint on the control input bound of a DC–DC boost converter. These characteristics make this converter to challenging case for researchers.

Although, linear controllers such as PI and PID present desirable performance in selected operation point. However, when the operation point is changed, their voltage regulation quality will decrease [8, 9]. So, some papers have suggested linear controller with adaptive coefficients but the complicated structure of this controller made it unattractive [10]. Another group of controllers that do not need exact information of mathematical model of system are intelligent controllers such as neural network [11] or fuzzy controllers [12]. However, because the use of these types of controllers requires considerable memory and computational efforts, their application in power electronics industry has not been welcomed [1]. Therefore,

✉ Alireza Khosravi, akhosravi@nit.ac.ir; Milad Malekzadeh, m.malekzade@stu.nit.ac.ir; Mehdi Tavan, m.tavan@srbiau.ac.ir | [1]Faculty of Electrical Engineering, Babol Noshirvani University of Technology, Babol, Iran. [2]Faculty of Electrical Engineering, Mahmudabad Branch, Islamic Azad University, Mahmudabad, Iran.

different studies have tried to eliminate mentioned weakness applying nonlinear controllers. In this regard, various nonlinear controller such as sliding mode [13–15], passivity-based control [8, 16] and backstepping control [17] have been suggested. However, this kind of controller requires an exact information of system states to present control effort and this drawback is significant. Because, when the converter is applied in noisy circumstance, the sensor cannot transfer exact information [18, 19]. Also, if the parameters of the system change drastically, the sensor performance will drop [20]. In order to unravel this problem, researchers have suggested observer. Observers could estimate required state and parameters using minimum sensor and sensorless control scheme will realize. High reliability, low cost and high efficiency make sensorless control scheme an application of interest in academy and industry [21].

In this regard, different observers are presented for DC–DC boost converter. Estimation of inductor current has been considered in [22]. In this paper, an observer is designed to estimate inductor current using input voltage and output voltage. This purpose has been improved in [23]. In this article, inductor current and input voltage have been estimated using output voltage. In addition, Estimation of inductor current has been considered in [21]. In this study, a unified observer is designed for a class of DC–DC converters such as DC–DC boost converter.

In this paper, a new nonlinear observer based on Immersion and Invariance (I&I) manifold is designed for DC–DC boost converter [23, 24]. The implementation of I&I based observer is simple and does need high gain to suppress nonlinear terms [24]. In addition, the observer does not require output injection error term to estimate unavailable states and parameters. The proposed observer estimates input voltage and resistive load using output voltage and inductor current. The exponential stability of the proposed observer is provided by Lyapunov stability theorem. Also, the closed-loop control stability is realized considering control input constraint. In order to obtain the gains of the observer, an improved particle optimization algorithm is considered. Particle swarm optimization algorithm is well-known algorithm in optimization problems and many researchers employ this algorithm in controller design [25–30]. However, by applying some modifications to the movement of particles towards the optimal solution, the accuracy and convergence rate of the algorithm is improved in proposed algorithm. In order to confirm the advantages of I&I based observer, its performance is compared with conventional observer [14]. Furthermore, to validate the effectiveness of the propped control scheme, the practical test is implemented in this article. Therefore, hardware-in-loop structure is designed using Advantech card to realize experimental test. The rest of paper is organized as follows:

Section 2 presents general definition of DC–DC boost converter. In Sect. 3, the proposed observer is designed according to immersion and invariance method and the comparison with conventional observer is presented in Sect. 4. The definition of the improved optimization algorithm is rendered in Sect. 5. Sections 6 and 7 demonstrate simulation and experimental results respectively and the paper ends with conclusion section.

2 Problem statement

The dynamic of DC–DC boost converter is presented in this section. DC–DC boost circuit is demonstrated in Fig. 1.

Where $y(t) \in \mathbb{R}$ is the output (capacitor) voltage, $x(t) \in \mathbb{R}$ is the input (inductor) current, $u \in (0, 1]$ is the continuous control signal ($u = 1 - \mu$), and C, L, G and E are positive constants representing the capacitance, inductance, load conductance and input voltage, respectively. Our aim is to regulate the output voltage to a desired value $V_d \geq E$. The average model of this converter is defined as follows [22]

$$\begin{aligned} C\dot{y} &= ux - Gy \\ L\dot{x} &= E - uy \end{aligned} \tag{1}$$

According to presented dynamic, observer will be designed in next section.

3 Observer design

In order to design observer according to immersion and invariance (I&I) method, *off-the-manifold* coordinate is defined as follows [22, 23]

$$\begin{aligned} z_1 &= \lambda_1 - G + \beta_1(\mathrm{y}, \mathrm{x}) \\ z_2 &= \lambda_2 - E + \beta_2(\mathrm{y}, \mathrm{x}) \end{aligned} \tag{2}$$

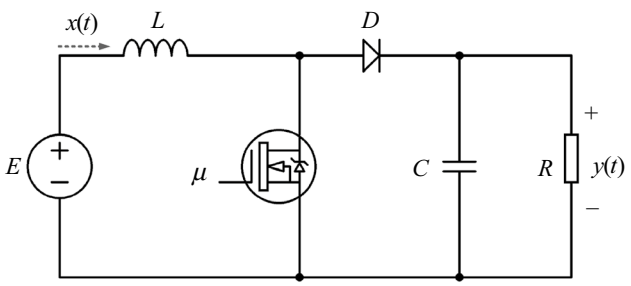

Fig. 1 DC–DC boost converter circuit

It is worth noting that λ_1, λ_2 are observer state and $\beta_1(y,x)$, $\beta_2(y,x)$ are smooth mapping yet to be defined. It is evident if $z = col(z_1, z_2)$ converges to zero, the estimations of output resistance and input voltage are obtained as follows

$$\begin{aligned}\hat{G} &= \lambda_1 + \beta_1(y,x)\\ \hat{E} &= \lambda_2 + \beta_2(y,x)\end{aligned} \tag{3}$$

The dynamic of $z = col(z_1, z_2)$ are achieved as follows

$$\begin{aligned}\dot{z}_1 &= \dot{\lambda}_1 + \frac{\partial \beta_1}{\partial y}\left(\frac{u}{C}x - \frac{G}{C}y\right) + \frac{\partial \beta_1}{\partial x}\left(\frac{E}{L} - \frac{u}{L}y\right)\\ \dot{z}_2 &= \dot{\lambda}_2 + \frac{\partial \beta_2}{\partial y}\left(\frac{u}{C}x - \frac{G}{C}y\right) + \frac{\partial \beta_2}{\partial x}\left(\frac{E}{L} - \frac{u}{L}y\right)\end{aligned} \tag{4}$$

Substituting the (2) in (4), we have:

$$\begin{aligned}\dot{z}_1 &= \dot{\lambda}_1 + \frac{\partial \beta_1}{\partial y}\left(\frac{u}{C}x - \frac{(\lambda_1 + \beta_1 - z_1)}{C}y\right) + \frac{\partial \beta_1}{\partial x}\left(\frac{(\lambda_2 + \beta_2 - z_2)}{L} - \frac{u}{L}y\right)\\ \dot{z}_2 &= \dot{\lambda}_2 + \frac{\partial \beta_2}{\partial y}\left(\frac{u}{C}x - \frac{(\lambda_1 + \beta_1 - z_1)}{C}y\right) + \frac{\partial \beta_2}{\partial x}\left(\frac{(\lambda_2 + \beta_2 - z_2)}{L} - \frac{u}{L}y\right)\end{aligned} \tag{5}$$

If the observer dynamic is defined

$$\begin{aligned}\dot{\lambda}_1 &= -\frac{\partial \beta_1}{\partial y}\left(\frac{u}{C}x - \frac{(\lambda_1 + \beta_1)}{C}y\right) - \frac{\partial \beta_1}{\partial x}\left(\frac{(\lambda_2 + \beta_2)}{L} - \frac{u}{L}y\right)\\ \dot{\lambda}_2 &= -\frac{\partial \beta_2}{\partial y}\left(\frac{u}{C}x - \frac{(\lambda_1 + \beta_1)}{C}y\right) - \frac{\partial \beta_2}{\partial x}\left(\frac{(\lambda_2 + \beta_2)}{L} - \frac{u}{L}y\right)\end{aligned} \tag{6}$$

We have

$$\begin{aligned}\dot{z}_1 &= \frac{\partial \beta_1}{\partial y}\frac{y}{C}z_1 - \frac{\partial \beta_1}{\partial x}\frac{z_2}{L}\\ \dot{z}_2 &= \frac{\partial \beta_2}{\partial y}\frac{y}{C}z_1 - \frac{\partial \beta_2}{\partial x}\frac{z_2}{L}\end{aligned} \tag{7}$$

Now, the Lyapunov function is defined as follows:

$$V(z) = \frac{1}{2}(z_1^2 + z_2^2) \tag{8}$$

time derivative along (8) yields

$$\dot{V}(z) = z_1\dot{z}_1 + z_2\dot{z}_2 = \frac{\partial \beta_1}{\partial y}\frac{y}{C}z_1^2 - \frac{\partial \beta_1}{\partial x}\frac{z_1 z_2}{L} + \frac{\partial \beta_2}{\partial y}\frac{y}{C}z_1 z_2 - \frac{\partial \beta_2}{\partial x}\frac{z_2^2}{L} \tag{9}$$

If the mapping function $\beta = col(\beta_1, \beta_2)$ is defined appropriately, we can conclude the stability of the proposed scheme. Considering $\beta_1 = -\alpha_1 y$ and $\beta_2 = \alpha_2 x$ $(\alpha_1, \alpha_2 > 0)$, we have

$$\dot{V}(z) = -\alpha_1\frac{y}{C}z_1^2 - \alpha_2\frac{z_2^2}{L} \le -\alpha_3(z_1^2 + z_2^2) \le -\frac{\alpha_3}{2}(z_1^2 + z_2^2) \le -\alpha_3 V(z) \tag{10}$$

where $\alpha_3 = \min(\alpha_1\frac{y}{C}, \frac{\alpha_2}{L})$. From (10), the exponential stability of the estimation error is proven. Therefore, the observer dynamic is achieved as follow

$$\begin{aligned}\dot{\lambda}_1 &= \alpha_1\left(\frac{u}{C}x - \frac{(\lambda_1 - \alpha_1 y)}{C}y\right)\\ \dot{\lambda}_2 &= -\alpha_2\left(\frac{(\lambda_2 + \alpha_2 x)}{L} - \frac{u}{L}y\right).\end{aligned} \tag{11}$$

4 Comparison and discussion

In this section, the performance of the proposed observer is compared with conventional observer that has been presented in [14]

$$\begin{aligned}\dot{\hat{y}} &= \frac{u\hat{x}}{C} - \frac{\hat{G}y}{C} + k_1(y - \hat{y})\\ \dot{\hat{x}} &= \frac{\hat{E}}{L} - \frac{u\hat{y}}{L} + k_2(x - \hat{x})\end{aligned} \tag{12}$$

where $k_1, k_2 > 0$.The input voltage and resistive load are obtained from following adaption law

$$\begin{aligned}\dot{\hat{E}} &= \gamma_1(x - \hat{x})\\ \dot{\hat{G}} &= -\gamma_2 y(y - \hat{y})\end{aligned} \tag{13}$$

where $\gamma_1, \gamma_2 > 0$. As can be seen, the conventional observer needs injection terms with high gain for acceptable performance while I&I technique does not need it. In addition, this observer needs 4 equations to estimate input voltage and load resistive while the proposed observer estimate unavailable parameters by 2 equations and the I&I observer order is less than conventional observer. Also, the practical implementation of the proposed observer is simpler in comparison with observer in [14].

In order to compare the performance of these observers, the closed-loop control scheme is implemented considering control input as

$$u = sat\left(\frac{\hat{E}}{V_d}\right) \tag{14}$$

If the voltage regulation errors are defined as $\tilde{y} = y - y_d$ and $\tilde{x} = x - x_d$ $(y_d = V_d,\ x_d = \frac{V_d^2 G}{E})$, we have

$$C\dot{\tilde{y}} = sat\left(\frac{\hat{E}}{y_d}\right)(\tilde{x} + x_d) - G(\tilde{y} + y_d)$$
$$L\dot{\tilde{x}} = E - sat\left(\frac{\hat{E}}{y_d}\right)(\tilde{y} + y_d) \quad (15)$$

The estimation error is defined as $\bar{E} = E - \hat{E}$. So

$$C\dot{\tilde{y}} = sat\left(\frac{E - \bar{E}}{y_d}\right)(\tilde{x} + x_d) - G(\tilde{y} + y_d)$$
$$L\dot{\tilde{x}} = E - sat\left(\frac{E - \bar{E}}{y_d}\right)(\tilde{y} + y_d) \quad (16)$$

Due to exponential convergence of the estimation error, we have

$$C\dot{\tilde{y}} = \frac{E}{y_d}\tilde{x} - G\tilde{y}$$
$$L\dot{\tilde{x}} = -\frac{E}{y_d}\tilde{y} \quad (17)$$

Which the characteristic equation $LCy_d^2\lambda^2 + LGy_d^2\lambda + E^2 = 0$ confirms the exponential of the voltage regulation error.

5 Improved particle swarm optimization algorithm (IPSO)

Particle swarm optimization is a social search algorithm modeled on the basis of the social behavior of bird flocks [24]. In the structure of this algorithm, each solution, which is called a particle, is equivalent to a bird. At the beginning of the algorithm, the particles flow in the search space. The particle movement in the search space is influenced by the experience and knowledge of themselves and their neighbors. Therefore, the position of the remainder of the particle swarm affects how a particle is searched. The result of the modeling of this social behavior is a search process in which particles tend toward successful regions. Particles learn from each other and go towards their best neighbors based on their knowledge. The particle optimization algorithm is based on the principle that at any given moment, each particle adjusts its place in the search space according to the best place ever reached to and the best place in its entire neighborhood. In the structure of this algorithm, a group of birds is randomly looking for food in the space. There is only one piece of food in the considered space. None of the birds knows where the food is. One of the best strategies can be to follow the bird that has the shortest distance to the food. This strategy is in fact the source of the algorithm. Each particle has a fitness value calculated trough a fitness function. The closer the particle to the target (food in the model of the movement of birds) in the search space is, the more it fitness is. Each particle also has a velocity that guides the particle's motion. Each particle continues its motion by following the optimal particles in the current state. In this way, a group of particles is created randomly at the beginning of the algorithm and tries to optimize the solution by updating the generations. In each step, each particle is updated using the two best values. The first is the best position ever reached by the particle. This location is stored and maintained, which is named *Pbest*. The other best value is the best position ever reached by the particle population. This position is represented as *gbest*. After finding the best values, the velocity and position of each particle are updated using Eqs. (1) and (2) [26].

$$v = w \times v + c_1 \times rand \times (pbest - position) + c_2 \times rand \times (gbest - position) \quad (18)$$

$$position = position + v \quad (19)$$

In the improved particle swarm optimization algorithm, an elimination period has been added to its classical form. At the beginning of each period, a specific number of the worst solutions will be eliminated and replaced by new solutions in the new search space. Creating new initial populations makes the particles find new paths to reach the best solution (gbest). These changes in the algorithm reduces the possibility of reaching local minima and increases the speed of finding optimal solutions. The steps of implementing the improved particle swarm optimization algorithm are as follows.

1. Select an initial search space suitable for the parameters of each particle, the initial population, the maximum number of iterations, c_1, c_2, w, ep (Elimination period. This parameter has been added to the classical algorithm and is determined based on the number of iterations) and et (Elimination percentage. This parameter has been added to the classical algorithm and is determined based on the percentage of the initial population).
2. Create the initial population in the search space.
3. Calculate the fitness function for each particle.
4. Determine *pbest* of each particle and *gbest*.
5. If the number of iterations is a multiple of ep, then make the following changes (elimination step):
   - 5.1 If the value of the parameters of each particle is greater than a threshold, add a unit to the search space of that particle member. (The threshold is a percentage of the maximum or minimum of the search space, and the value is arbitrary).
   - 5.2 Determine et percent of the initial population that has the worst fitness function.

5.3 Eliminate the selected et percent and create a new population in the new search space. The velocity (v) of the new particles is selected to be zero.
5.4 Calculate the fitness function for the new particles.
5.5 Determine *pbest* for each particle and *gbest*.

6. Update the position of all the particles using Eqs. (10) and (11).
7. Go to step 3 and repeat steps (3, 4, 5, 6, and 7) until satisfying the termination conditions.

The effectiveness of the proposed optimization algorithm is proven in [25, 26]. The flowchart of the proposed algorithm is presented in Fig. 2.

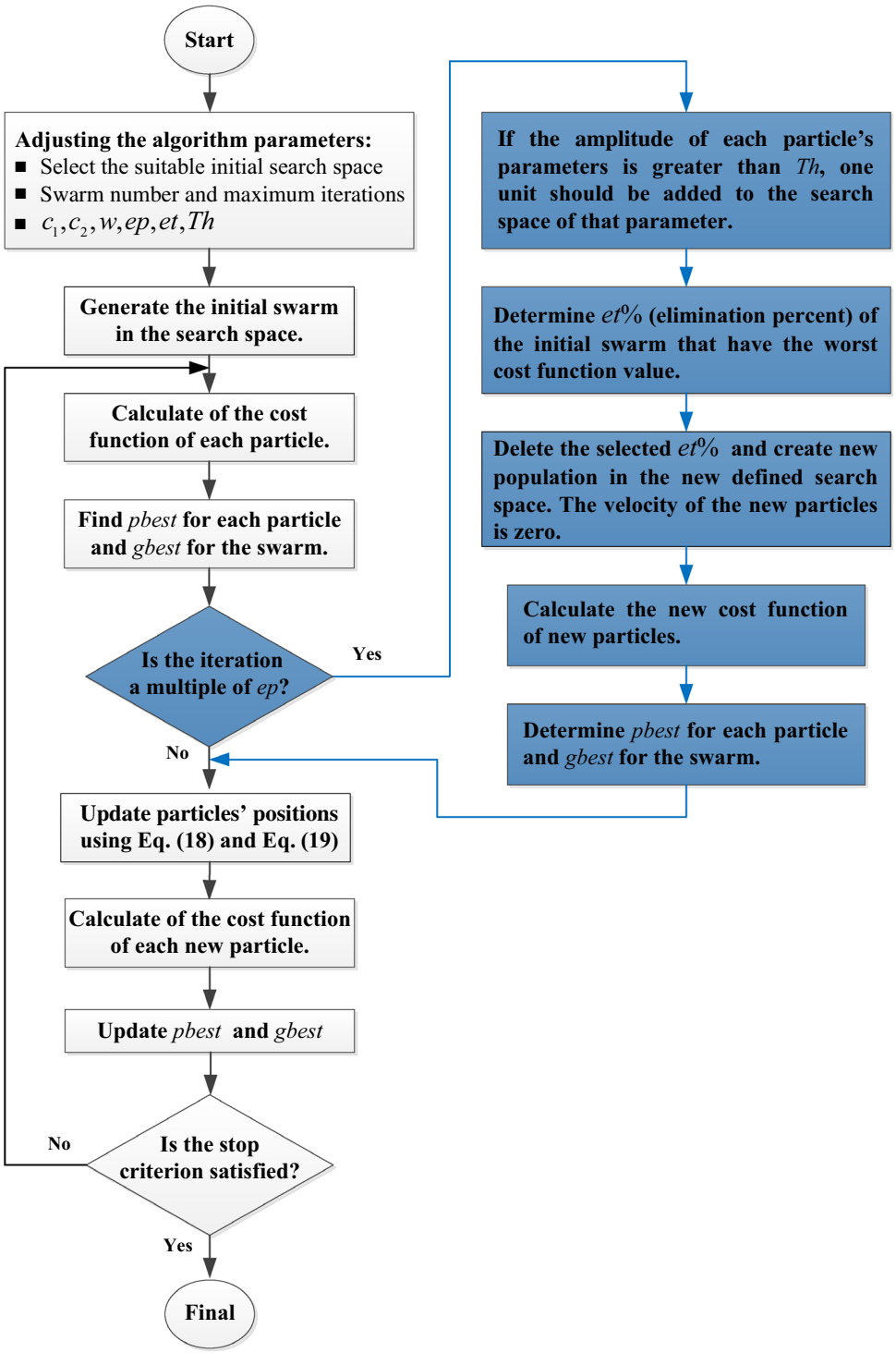

Fig. 2 The flowchart of IPSO

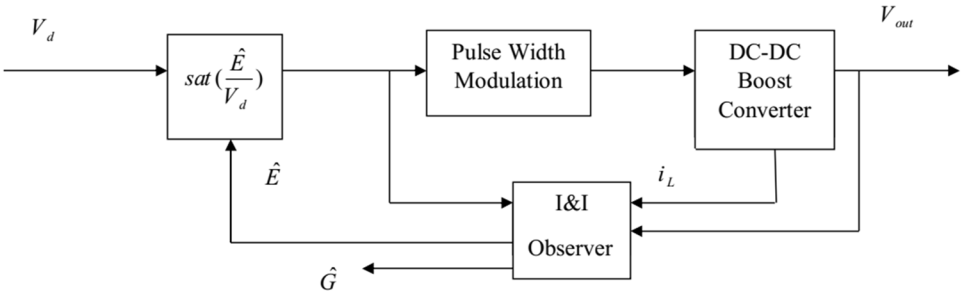

Fig. 3 The block diagram of the proposed control scheme

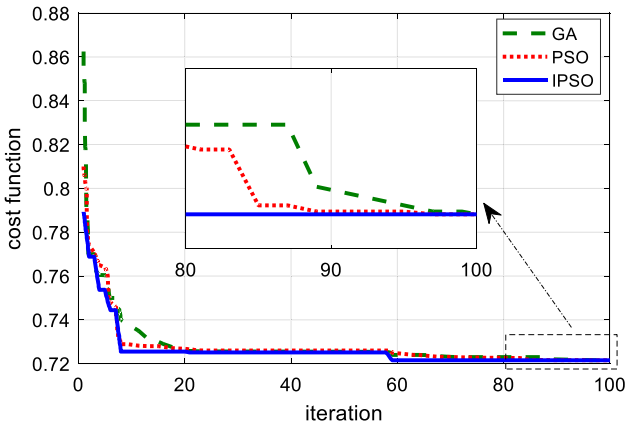

Fig. 4 The convergence trajectory of the cost function using IPSO in comparison with PSO and GA

6 Simulation results

In this section, the performance of the proposed observer is compared with observer in [14]. In order to realize real conditions, voltage drop along DC–DC boost converter such as inductor resistance and non-ideal diode is considered. Also, Simulation results is implemented in Power Gui/Simulink/MATLAB. The block diagram of the proposed control scheme is depicted in Fig. 3.

The parameters of the circuit are considered as follows:$L = 3.5\,\text{mH}$, $C = 330\,\mu\text{F}$, $R = 120\,\Omega$. In order to achieve optimal gains of observer, the input voltage and desired voltage are defined 10 V and 15 V respectively. The cost function is considered as follows

$$J = \int_0^t (\tilde{y}^2)dt \tag{20}$$

The optimization result is depicted in Fig. 4.

According to optimization process, the observer gains are achieved as follows: $a_1 = 0.5447$, $a_2 = 0.2348$. Also, the conventional observer gains are obtained as follows: $k_1 = 245.6348, k_2 = 293.7209, \gamma_1 = 101.5723, \gamma_2 = 64.281.1$ The simulation is implemented according to two conditions. At the first, the input voltage is defined 10 V and is changed to 7 V at t = 0.5 s. Also, the reference voltage is considered 15 V (Figs. 5, 6).

As can be seen, the performance of the proposed observer is better than observer in [14]. The proposed observer presents lower overshoot and faster convergence. Specially, the estimation of output load is significantly better in comparison with [14] due to its lower gains. It is worth noting that due to voltage drop along converter, the observer estimates input voltage lower than real value to compensate this weakness in control input. In second condition, the input voltage is assumed constant 10 V. However resistive load is changed to $R = 60\,\Omega$. The results is depicted in Figs. 7 and 8.

Similar to previous condition, the response of the proposed control scheme is better than observer in [14].

7 Experimental test

In this section, the efficiency of the proposed scheme is validated via experimental implementation. The experimental testbed is depicted in Fig. 9.

In order to realize practical test, a data acquisition card called Advantech card 1710 HG is employed. Advantech

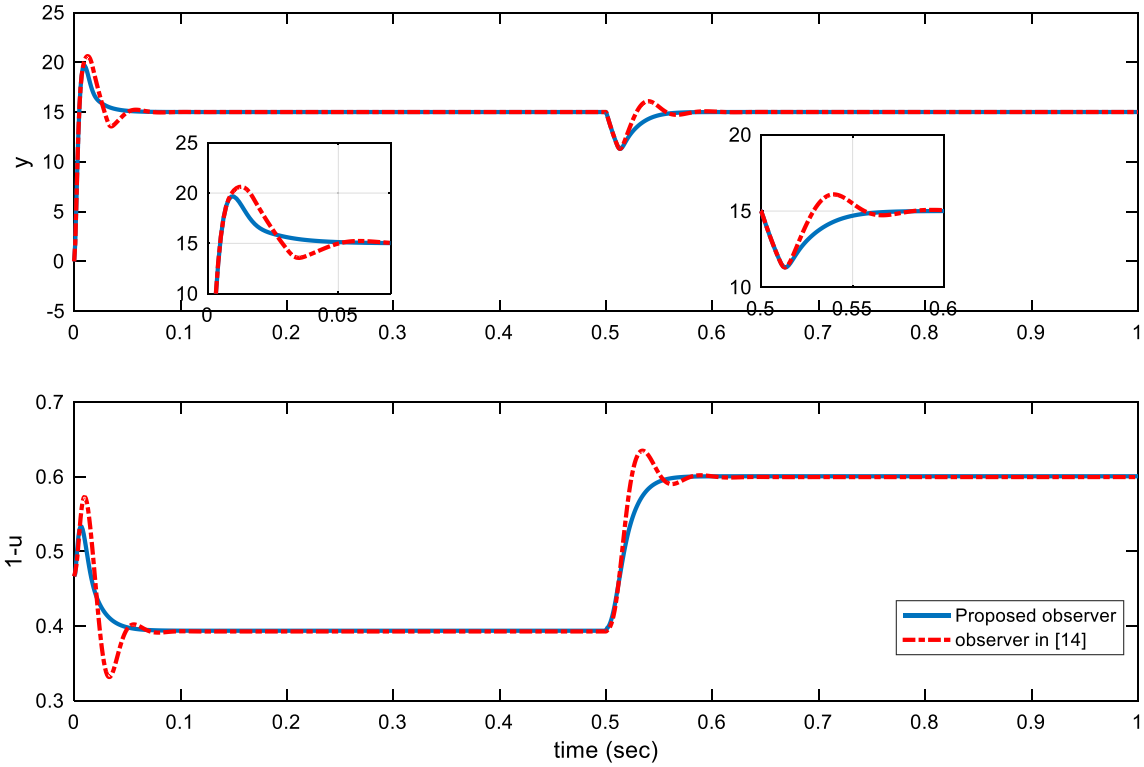

Fig. 5 The performance of the proposed control scheme in the presence of input voltage variation

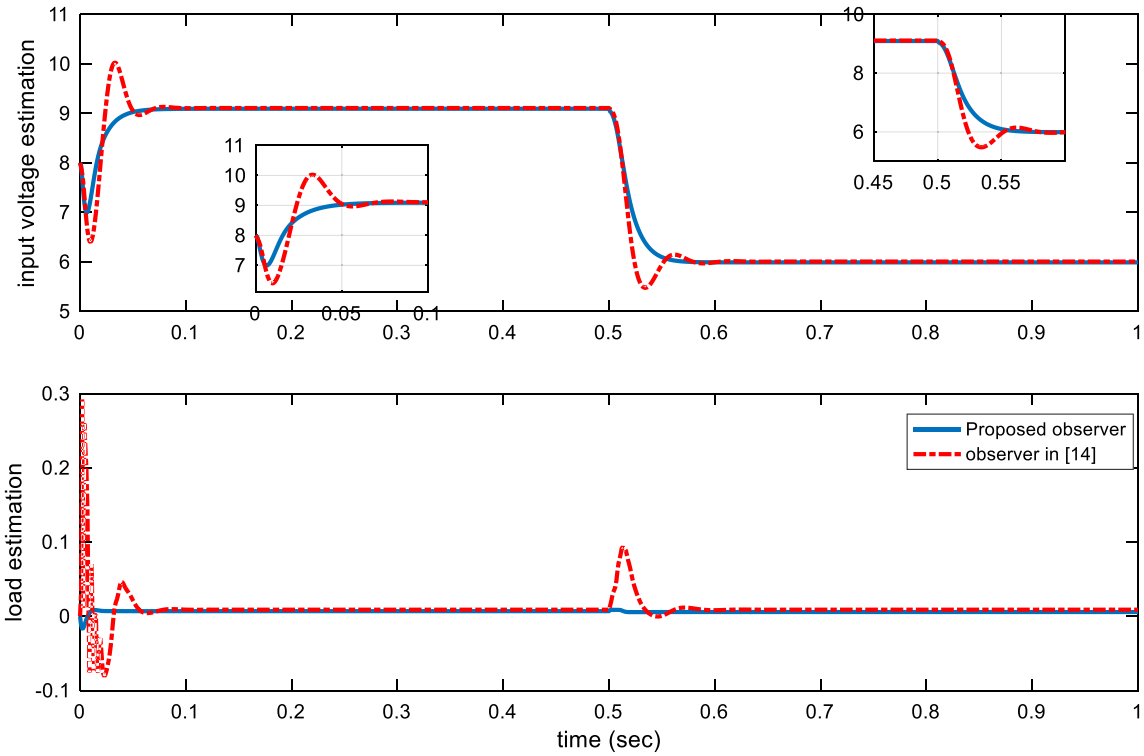

Fig. 6 The performance of the proposed observer in the presence of input voltage variation

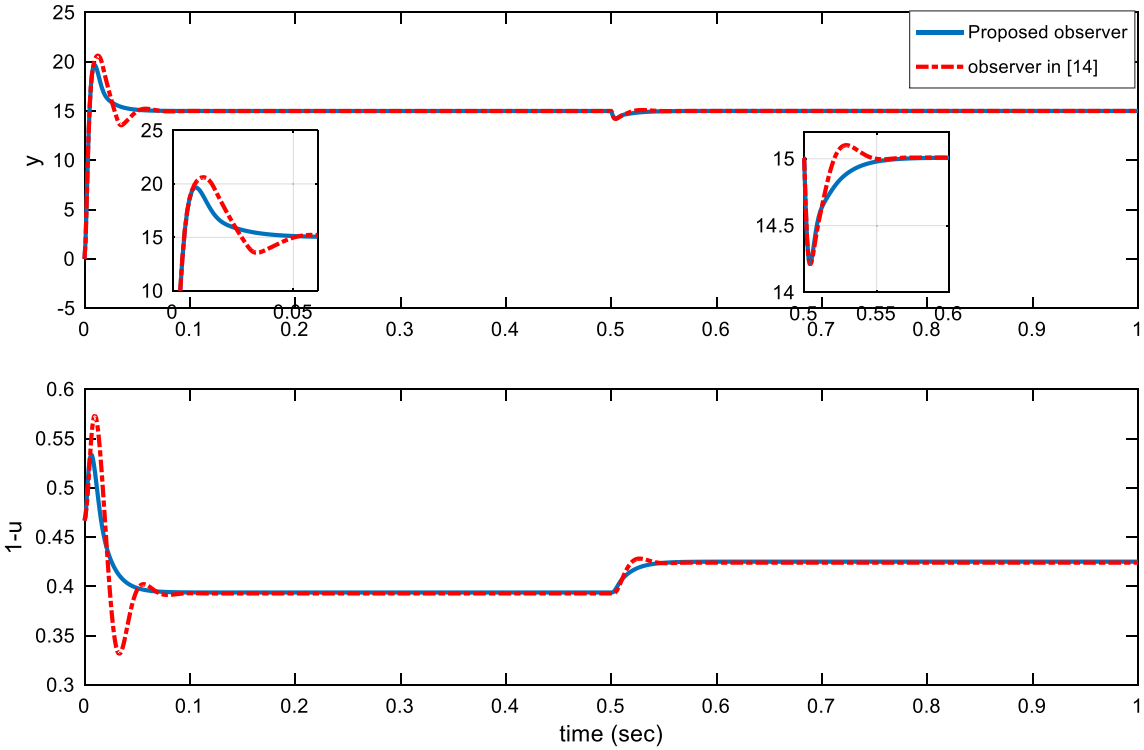

Fig. 7 The performance of the proposed control scheme in the presence of load variation

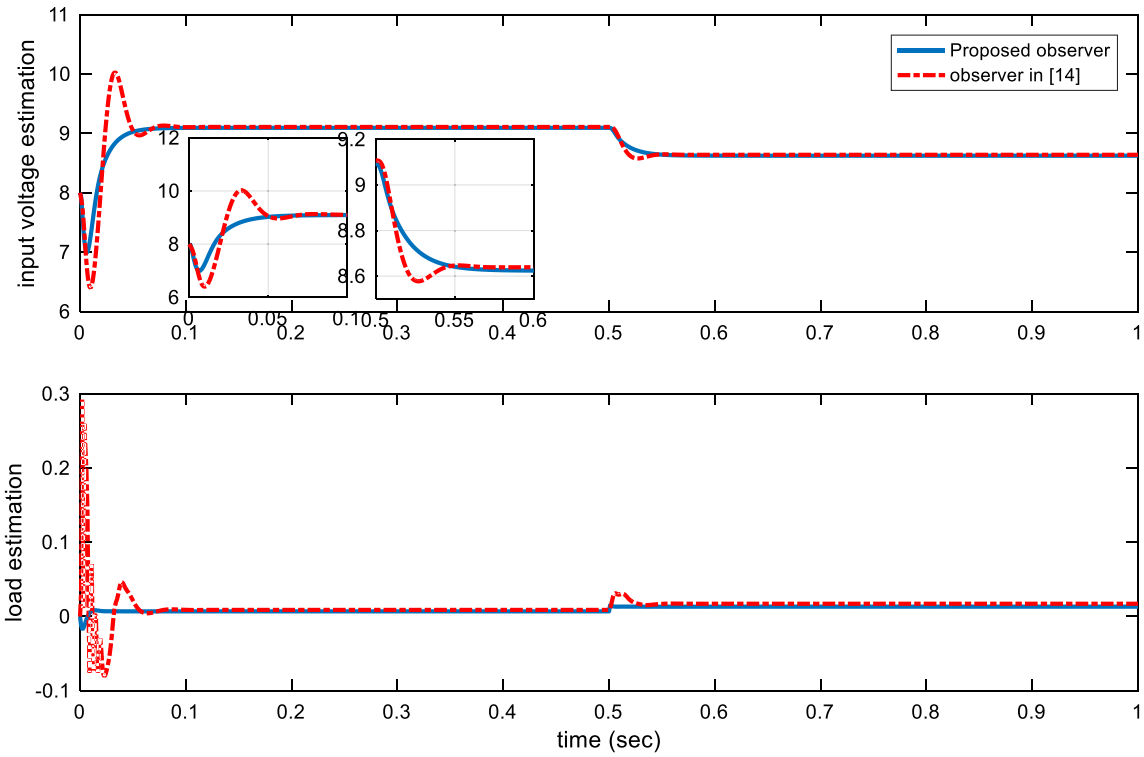

Fig. 8 The performance of the proposed observer in the presence of load variation

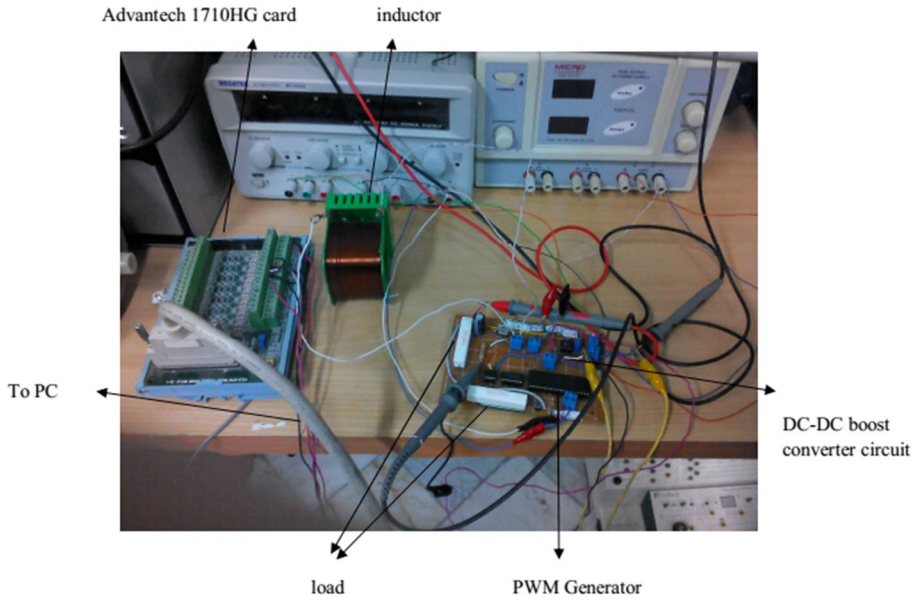

Fig. 9 Experiment set of prototype DC–DC boost converter with the proposed controller

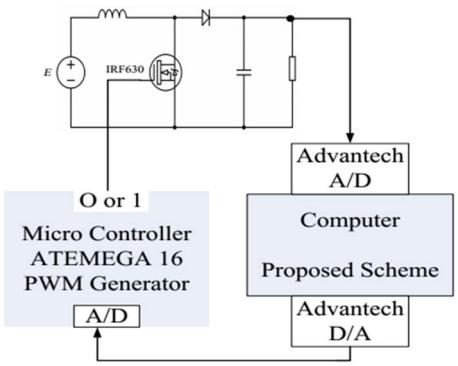

Fig. 10 Overview of hardware-in-loop implementation

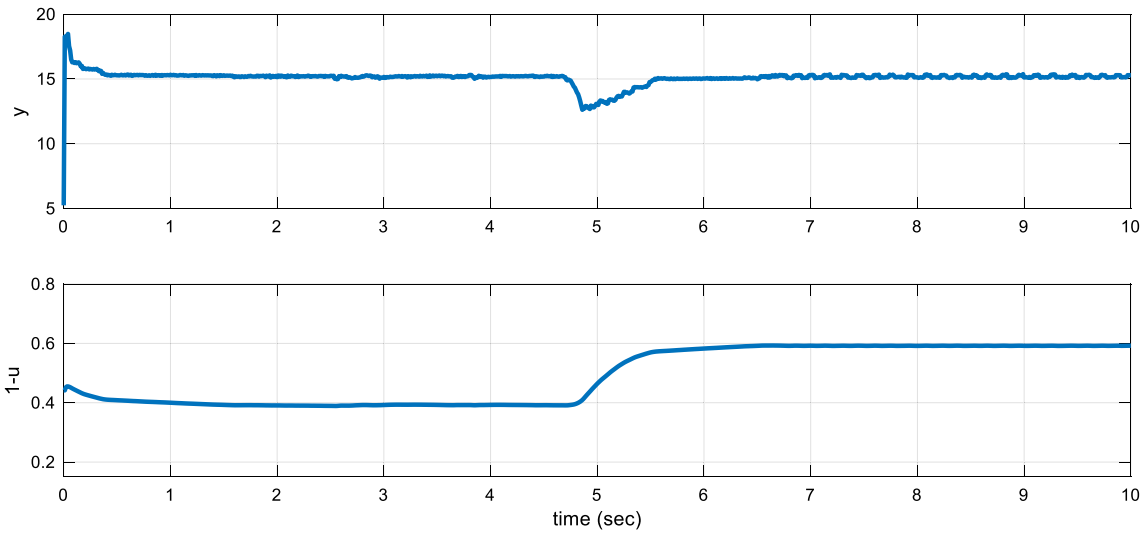

Fig. 11 Experimental results for a change in the input voltage from E = 10–7 V

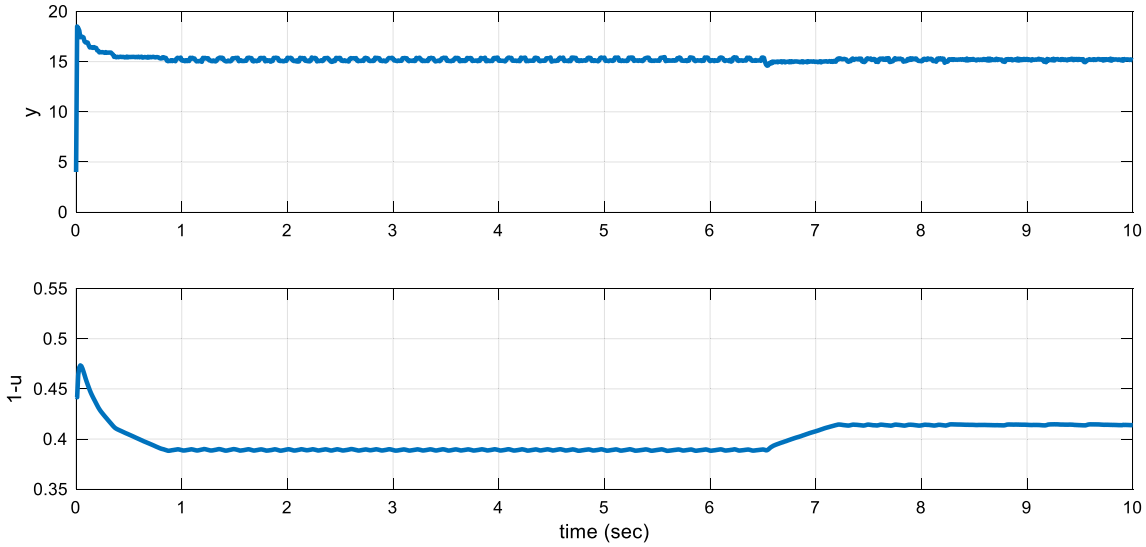

Fig. 12 Experimental results for a change in the load from R = 120 to 60 Ω

1710 HG is a multi-function data acquisition card with full capabilities to acquire data and, of course, for control purposes [31]. The proposed method is programmed in Simulink/MATLAB with Real Time Windows Target and the output of Advantech card is inserted into PWM (Pulse Width Modulation) with 20 k Hz switching frequency. The structure of the practical test is given in Fig. 10.

The practical scenario is similar to simulation results and the experimental results are depicted in Figs. 11 and 12.

As can be seen, the practical results confirm the capability of the proposed method in real time application.

8 Conclusion

In this study, a new nonlinear observer is presented for DC–DC boost converter. This observer is designed based on Immersion and Invariance technique with exponential stability. The proposed observer can estimate the input voltage and resistive load using output voltage and inductor current. In order to tune the observer gains, an improved particle optimization algorithm is employed. The effectiveness of this method is compared with conventional observer and the simulation results endorse the advantages of the proposed nonlinear observer. Also, the experimental test is implemented to confirm the capability of the proposed method in real time application.

Compliance with ethical standards

Conflict of interest The authors declare that they have no competing interests.

Appendix

In order to generate PWM structure, ATMEGA32 has been employed. Following code has been programmed for this purpose.

```
/*************************************/
This program was created by the CodeWizardAVR V3.12 Advanced Automatic Program Generator
Chip type           : ATmega32
Program type        : Application
AVR Core Clock frequency: 8.000000 MHz
Memory model        : Small
External RAM size   : 0
Data Stack size     : 512
/*************************************************************
#include <mega32.h>
#include <delay.><
 //Declare your global variables here
unsigned int x=240;
 //Timer 0 overflow interrupt service routine
interrupt [TIM0_OVF] void timer0_ovf_isr(void(
{

 //Reinitialize Timer 0 value
TCCR0=(0<<WGM00) | (0<<COM01) | (0<<COM00) | (0<<WGM01) | (0<<CS02) | (0<<CS01) | (0<<CS00);
TCNT0=206;
 //Place your code here
OCR0=x;
TCCR0=(1<<WGM00) | (1<<COM01) | (1<<COM00) | (1<<WGM01) | (0<<CS02) | (1<<CS01) | (0<<CS00);
}
 // Voltage Reference: Int., cap. on AREF
#define ADC_VREF_TYPE ((1<<REFS1) | (1<<REFS0) | (1<<ADLAR))

 //Read the 8 most significant bits
 //of the AD conversion result
unsigned char read_adc(unsigned char adc_input)
{
ADMUX=adc_input | ADC_VREF_TYPE;
 //Delay needed for the stabilization of the ADC input voltage
delay_us(10);
 //Start the AD conversion
ADCSRA|=(1<<ADSC);
 //Wait for the AD conversion to complete
while ((ADCSRA & (1<<ADIF))==0);
ADCSRA|=(1<<ADIF);
return ADCH;
}
void main(void(
{
 //Declare your local variables here
 //Input/Output Ports initialization
 //Port A initialization
 //Function: Bit7=In Bit6=In Bit5=In Bit4=In Bit3=In Bit2=In Bit1=In Bit0=In
DDRA=(0<<DDA7) | (0<<DDA6) | (0<<DDA5) | (0<<DDA4) | (0<<DDA3) | (0<<DDA2) | (0<<DDA1) | (0<<DDA0);
 //State: Bit7=T Bit6=T Bit5=T Bit4=T Bit3=T Bit2=T Bit1=T Bit0=T
PORTA=(0<<PORTA7) | (0<<PORTA6) | (0<<PORTA5) | (0<<PORTA4) | (0<<PORTA3) | (0<<PORTA2) | (0<<PORTA1) | (0<<PORTA0);
 //Port B initialization
 //Function: Bit7=In Bit6=In Bit5=In Bit4=In Bit3=Out Bit2=In Bit1=In Bit0=In
 DDRB=(0<<DDB7) | (0<<DDB6) | (0<<DDB5) | (0<<DDB4) | (1<<DDB3) | (0<<DDB2) | (0<<DDB1) | (0<<DDB0):
 //State: Bit7=T Bit6=T Bit5=T Bit4=T Bit3=0 Bit2=T Bit1=T Bit0=T
PORTB=(0<<PORTB7) | (0<<PORTB6) | (0<<PORTB5) | (0<<PORTB4) | (0<<PORTB3) | (0<<PORTB2) | (0<<PORTB1) | (0<<PORTB0);
 //Port C initialization
 //Function: Bit7=In Bit6=In Bit5=In Bit4=In Bit3=In Bit2=In Bit1=In Bit0=In
DDRC=(0<<DDC7) | (0<<DDC6) | (0<<DDC5) | (0<<DDC4) | (0<<DDC3) | (0<<DDC2) | (0<<DDC1) | (0<<DDC0);
 //State: Bit7=T Bit6=T Bit5=T Bit4=T Bit3=T Bit2=T Bit1=T Bit0=T
PORTC=(0<<PORTC7) | (0<<PORTC6) | (0<<PORTC5) | (0<<PORTC4) | (0<<PORTC3) | (0<<PORTC2) | (1<<PORTC1) | (1<<PORTC0);
```

```
 //Port D initialization
 //Function: Bit7=Out Bit6=Out Bit5=Out Bit4=Out Bit3=Out Bit2=Out Bit1=Out Bit0=Out
DDRD=(0<<DDD7) | (0<<DDD6) | (0<<DDD5) | (0<<DDD4) | (0<<DDD3) | (0<<DDD2) |
(0<<DDD1) | (0<<DDD0):
 //State: Bit7=0 Bit6=0 Bit5=0 Bit4=0 Bit3=0 Bit2=0 Bit1=0 Bit0=0
PORTD=(0<<PORTD7) | (0<<PORTD6) | (0<<PORTD5) | (0<<PORTD4) | (0<<PORTD3) |
(0<<PORTD2) | (0<<PORTD1) | (0<<PORTD0):

 //Timer/Counter 0 initialization
 //Clock source: System Clock
 //Clock value: 1000.000 kHz
 //Mode: Fast PWM top=0xFF
 //OC0 output: Inverted PWM
 //Timer Period: 0.256 ms
 //Output Pulse(s):
 //OC0 Period: 0.256 ms Width: 0.256 ms
TCCR0=(1<<WGM00) | (1<<COM01) | (1<<COM00) | (1<<WGM01) | (0<<CS02) |
(1<<CS01) | (0<<CS00);
TCNT0=206;
OCR0=x;

 //Timer(s)/Counter(s) Interrupt(s) initialization
TIMSK=(0<<OCIE2) | (0<<TOIE2) | (0<<TICIE1) | (0<<OCIE1A) | (0<<OCIE1B) |
(0<<TOIE1) | (0<<OCIE0) | (1<<TOIE0):

 //Analog Comparator initialization
 //Analog Comparator: Off
 //The Analog Comparator's positive input is
 //connected to the AIN0 pin
 //The Analog Comparator's negative input is
 //connected to the AIN1 pin
ACSR=(1<<ACD) | (0<<ACBG) | (0<<ACO) | (0<<ACI) | (0<<ACIE) | (0<<ACIC) |
(0<<ACIS1) | (0<<ACIS0);

 //ADC initialization
 //ADC Clock frequency: 1000.000 kHz
 //ADC Voltage Reference: Int., cap. on AREF
 //ADC Auto Trigger Source: ADC Stopped
 //Only the 8 most significant bits of
 //the AD conversion result are used
ADMUX=ADC_VREF_TYPE;
ADCSRA=(1<<ADEN) | (0<<ADSC) | (0<<ADATE) | (0<<ADIF) | (0<<ADIE) | (0<<ADPS2) |
(1<<ADPS1) | (1<<ADPS0);
SFIOR=(0<<ADTS2) | (0<<ADTS1) | (0<<ADTS0);

 //Global enable interrupts
#asm("sei")

while (1(
     {
 //     Place your code here
   x=read_adc(1)
   if(x>=97)
   x=97;
     if(x<=1)
   x=1;

       x=x/2+206;
     }
     }
```

References

1. Yazici İ, Yaylaci EK (2016) Fast and robust voltage control of DC–DC boost converter by using fast terminal sliding mode controller. IET Power Electron 9(1):120–125
2. Cheng L, Acuna P, Aguilera RP, Jiang J, Wei S, Fletcher J, Lu DDC (2017) Model predictive control for DC–DC boost converters with reduced-prediction horizon and constant switching frequency. IEEE Trans Power Electron 33:9064–9075
3. Pourmousa N, Ebrahimi SM, Malekzadeh M, Alizadeh M (2019) Parameter estimation of photovoltaic cells using improved Lozi map based chaotic optimization algorithm. Sol Energy 180:180–191
4. Rakhtala SM, Shafiee Roudbari E (2016) Fuzzy PID control of a stand-alone system based on PEM fuel cell. Int J Electr Power Energy Syst 78:576–590
5. Camara MB, Gualous H, Gustin F, Berthon A (2008) Design and new control of DC/DC converters to share energy between supercapacitors and batteries in hybrid vehicles. IEEE Trans Veh Technol 57(5):2721–2735
6. Wang YX, Yu DH, Kim YB (2014) Robust time-delay control for the DC–DC boost converter. IEEE Trans Industr Electron 61(9):4829–4837
7. Yazici İ (2014) Robust voltage-mode controller for DC–DC boost converter. IET Power Electron 8(3):342–349
8. Son YI, Kim IH (2012) Complementary PID controller to passivity-based nonlinear control of boost converters with inductor resistance. IEEE Trans Control Syst Technol 20(3):826–834
9. Alvarez-Ramirez J, Cervantes I, Espinosa-Perez G, Maya P, Morales A (2001) A stable design of PI control for DC–DC converters with an RHS zero. IEEE Trans Circuits Syst I Fundam Theory Appl 48(1):103–106
10. Shirazi M, Zane R, Maksimovic D (2009) An autotuning digital controller for DC–DC power converters based on online frequency-response measurement. IEEE Trans Power Electron 24(11):2578–2588
11. Wai RJ, Shih LC (2012) Adaptive fuzzy-neural-network design for voltage tracking control of a DC–DC boost converter. IEEE Trans Power Electron 27(4):2104–2115
12. El Beid S, Doubabi S (2014) DSP-based implementation of fuzzy output tracking control for a boost converter. IEEE Trans Ind Electron 61(1):196–209
13. Vidal-Idiarte E, Carrejo CE, Calvente J, Martínez-Salamero L (2011) Two-loop digital sliding mode control of DC–DC power converters based on predictive interpolation. IEEE Trans Ind Electron 58(6):2491–2501
14. Oucheriah S, Guo L (2013) PWM-based adaptive sliding-mode control for boost DC–DC converters. IEEE Trans Ind Electron 60(8):3291–3294
15. Lopez-Santos O, Martinez-Salamero L, Garcia G, Valderrama-Blavi H, Sierra-Polanco T (2015) Robust sliding-mode control design for a voltage regulated quadratic boost converter. IEEE Trans Power Electron 30(4):2313–2327
16. del Puerto-Flores D, Scherpen JM, Liserre M, de Vries MM, Kransse MJ, Monopoli VG (2014) Passivity-based control by series/parallel damping of single-phase PWM voltage source converter. IEEE Trans Control Syst Technol 22(4):1310–1322
17. Alvarez-Ramirez J, Espinosa-Pérez G, Noriega-Pineda D (2003) Current-mode control of DC–DC power converters: a backstepping approach. Int J Robust Nonlinear Control 13(5):421–442
18. Malekzadeh M, Khosravi A, Tavan M (2018) Observer based control scheme for DC–DC boost converter using sigma–delta modulator. COMPEL Int J Comput Math Electr Electron Eng 37(2):784–798
19. Malekzadeh M, Khosravi A, Tavan M (2019) Immersion and invariance-based filtered transformation with application to estimator design for a class of DC–DC converters. Trans Inst Meas Control 41(5):1323–1330
20. Malekzadeh M, Khosravi A, Tavan M (2019) A novel adaptive output feedback control for DC–DC boost converter using immersion and invariance observer. Evol Syst. https://doi.org/10.1007/s12530-019-09268-7
21. Malekzadeh M, Khosravi A, Tavan M (2019) A novel sensorless control scheme for DC–DC boost converter with global exponential stability. Eur Phys J Plus 134(7):338
22. Cho H, Yoo SJ, Kwak S (2014) State observer based sensor less control using Lyapunov's method for boost converters. IET Power Electron 8(1):11–19
23. Karagiannis D, Astolfi A, Ortega R (2003) Two results for adaptive output feedback stabilization of nonlinear systems. Automatica 39(5):857–866
24. Morbidi F, Mariottini GL, Prattichizzo D (2010) Observer design via immersion and invariance for vision-based leader–follower formation control. Automatica 46(1):148–154
25. Salahshour E, Malekzadeh M, Gholipour R, Khorashadizadeh S (2019) Designing multi-layer quantum neural network controller for chaos control of rod-type plasma torch system using improved particle swarm optimization. Evol Syst 10(3):317–331
26. Salahshour E, Malekzadeh M, Gordillo F, Ghasemi J (2018) Quantum neural network-based intelligent controller design for CSTR using modified particle swarm optimization algorithm. Transactions of the Institute of Measurement and Control, p 0142331218764566
27. Ebrahimi SM, Salahshour E, Malekzadeh M, Gordillo F (2019) Parameters identification of PV solar cells and modules using flexible particle swarm optimization algorithm. Energy 179:358–372
28. Gholipour R, Khosravi A, Mojallali H (2015) Multi-objective optimal backstepping controller design for chaos control in a rod-type plasma torch system using Bees Algorithm. Appl Math Model 39(15):4432–4444
29. Alfi A, Khosravi A, Lari A (2013) Swarm-based structure-specified controller design for bilateral transparent teleoperation systems via μ synthesis. IMA J Math Control Inf 31(1):111–136
30. Gholipour R, Khosravi A, Mojallali H (2012) Intelligent backstepping control for Genesio–Tesi chaotic system using a chaotic particle swarm optimization algorithm. Int J Comput Electr Eng 4(5):618
31. Salahshour E, Noei AR, Malekzadeh M (2014) A computerized and on-line super twisting speed control of alternating current asynchronous machine using Omron V1000® Drive. J Eng Technol 4(1):12–17